Terahertz induced transparency in single-layer graphene

Citation	Paul, M. J., Lee, B., Wardini, J. L., Thompson, Z. J., Stickel, A. D., Mousavian, A., ... & Lee, Y. S. (2014). Terahertz Induced Transparency in Single-Layer Graphene. Applied Physics Letters, 105(22), 221107. doi:10.1063/1.4902999
DOI	10.1063/1.4902999
Publisher	American Institute of Physics Publishing
Version	Version of Record
Terms of Use	http://cdss.library.oregonstate.edu/sa-termsofuse

Terahertz induced transparency in single-layer graphene

Michael J. Paul,[1] Byounghwak Lee,[1] Jenna L. Wardini,[1] Zachary J. Thompson,[1] Andrew D. Stickel,[1] Ali Mousavian,[1] Hyunyong Choi,[2] Ethan D. Minot,[1] and Yun-Shik Lee[1,a)]
[1]*Department of Physics, Oregon State University, Corvallis, Oregon 97331-6507, USA*
[2]*School of Electrical and Electronic Engineering, Yonsei University, Seoul, South Korea*

(Received 19 August 2014; accepted 17 November 2014; published online 2 December 2014)

We show that the transmission of a terahertz (THz) pulse through single-layer graphene is strongly nonlinear. As the peak electric field of the THz pulse exceeds 50 kV/cm, the graphene becomes increasingly transparent to the THz radiation. When field strength reaches 800 kV/cm, the increased transparency corresponds to a two-fold decrease in the time-average sheet conductivity of the graphene (time averaged over the duration of the pulse). Time-resolved measurements reveal that the leading portion of the pulse creates transparency for the trailing portion, with a 10-fold suppression in sheet conductivity at the tail of the strongest THz pulse. Comparing the THz-induced transparency phenomena in different sample geometries shows that substrate-free graphene is the best geometry for maximizing the nonlinear transparency effect. © *2014 AIP Publishing LLC*.
[http://dx.doi.org/10.1063/1.4902999]

Graphene is a promising electronic material for high speed electronic devices. Recently, 300-GHz graphene transistors and photodetectors have been demonstrated.[1–4] The predicted strong nonlinear responses of graphene in infrared (IR) and terahertz (THz) bands make it even more attractive because of its applications to active photonic devices.[5] As the operating frequency of graphene devices goes beyond 100 GHz, it becomes crucial to understand how this material behaves in the THz regime. As the internal electric field inside nanometer-scale devices could easily reach 100 kV/cm, it is also desirable to determine the nonlinear THz responses of graphene. In a weak optical field, graphene behaves linearly over a broad spectral range from visible to THz,[6–8] and the THz conductivity of graphene exhibits a Drude-like frequency dependence.[8–11] At present, only a few experiments on the high THz-field response of graphene have been reported: strong THz pulses enhance the transmission,[12–14] which has been attributed to increase of the electron temperature via carrier-carrier scattering. However, unlike THz-induced transparency in doped semiconductors which is caused by inter-valley scattering,[15,16] the underlying mechanisms of THz-induced transparency in graphene are largely unknown.

In this study, we present intensity dependent THz imaging and THz time-domain spectroscopy (THz-TDS) of two CVD-grown single-layer graphene samples. We demonstrate that strong THz pulses enhance transmission in graphene and the THz-induced transparency depends on spatial homogeneity of the graphene samples and the interface with its substrate. The experimental observations lead to a unique nonlinear THz property of graphene independent of spatial inhomogeneity and substrate material. Our study also investigates how the THz-induced transparency evolves in the time domain.

We studied two types of CVD graphene samples grown with different recipes: one sample has uniform graphene coverage,[17] and the other sample is inhomogeneous on the millimeter scale.[18] The graphene sheets were covered with PMMA and subsequently transferred onto two types of sample mounts: PMMA/graphene-on-Si (100-nm PMMA layer; inhomogeneous graphene) (Fig. 1(a)) and free-standing PMMA/graphene film (180-nm PMMA layer; homogeneous graphene) over 2-mm circular holes in an aluminum plate (Fig. 1(b)). PMMA is an uncharged polymer and contains

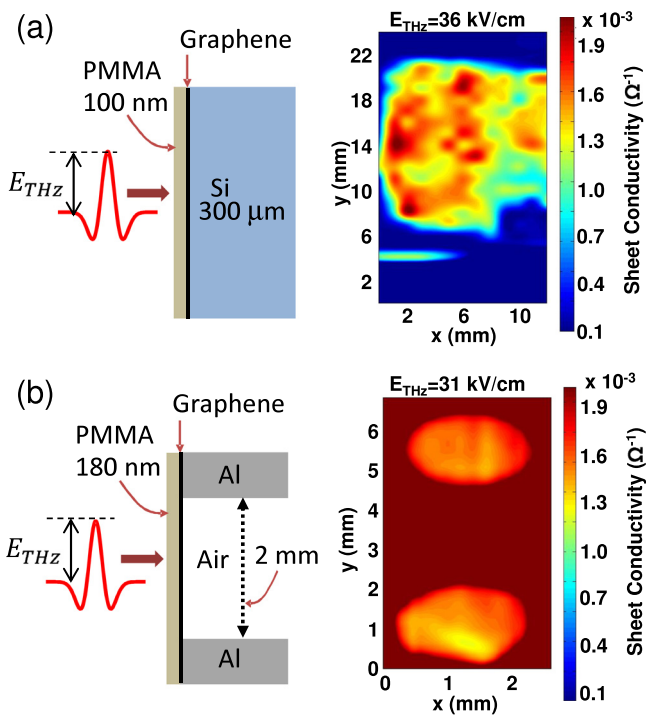

FIG. 1. Sheet conductivity images of (a) PMMA/graphene-on-Si (inhomogeneous) and (b) free-standing PMMA/graphene (homogeneous) samples at low THz intensity ($E_{THz} \sim 30$ kV/cm). Raster images were taken over (a) 25×13-mm^2 rectangle and (b) two 2-mm diameter holes with (a) 1-mm and (b) 0.2-mm pixel size. In the images, (a) the rectangular area of graphene is colored with cyan, yellow, and red, and (b) the circles of graphene are colored with yellow and orange.

a)Electronic mail: leeys@physics.oregonstate.edu

fewer charge traps than SiO_2, and hence the free-standing PMMA/graphene structure reduces parasitic substrate effects. THz absorption and interference in the PMMA thin films are negligible and the interface with PMMA induces small changes in the THz properties of graphene.[9]

We measured THz transmission through the graphene samples using broadband THz pulses (central frequency, 1 THz; bandwidth, 1 THz), while controlling THz intensity, sample position, and optical-probe delay time. The THz pulses were generated via optical rectification of femtosecond pulses with tilted pulse fronts in a MgO-doped $LiNbO_3$ prism.[19–21] The light source was a 1-kHz regenerative amplifier (wavelength, 800 nm; pulse energy, 1 mJ; pulse duration, 100 fs). THz pulses were focused to near diffraction limit onto the samples using parabolic mirrors (beam waist, 0.3 mm). THz pulse energy was measured by a liquid He cooled Si:Bolometer, and THz waveforms were determined by electro-optic sampling with a 150 -μm ZnTe crystal.

Figure 1 shows sheet conductivity, σ_s, images of the two graphene samples calculated from the THz transmission at low intensity ($E_{THz} \sim 30$ kV cm^{-1}) using the thin-film transmission coefficient for graphene on a substrate of refractive index n:

$$t(\sigma_s) = \frac{2}{n + 1 + Z_0\sigma_s}, \quad (1)$$

where $n = 3.42$ for the graphene-on-Si sample and $n = 1$ for the suspended graphene sample.[11] Z_0 (376.7 Ω) is the vacuum impedance. In Fig. 1(a), the rectangular area of cyan, yellow, and red indicates the graphene-on-Si, while Si and air are colored with dark blue. In Fig. 1(b), the circular regions of yellow and orange indicate the suspended graphene. The THz absorption reaches 20% in the graphene-on-Si sample and 40% in the suspended graphene sample. This THz absorption is an order of magnitude larger than graphene's optical absorption ($\pi\alpha \cong 2.3\%$, where α is the fine structure constant), which implies that intraband transitions dominate the interactions of THz waves with graphene.[9,11] As shown in Fig. 1(a), inhomogeneity on the millimeter length scale is observed in the graphene-on-Si sample. The sheet conductivity widely varies from 0.9 to 2.0×10^{-3} Ω^{-1}. Optical microscope images and Raman spectroscopy confirmed that the inhomogeneity mainly comes from incomplete graphene coverage. On the other hand, the suspended graphene layer is nearly uniform ($\sigma_s \cong 1.6 \times 10^{-3}$ Ω^{-1}) as shown in Fig. 1(b). The carrier density is estimated as $\sim 5 \times 10^{12}$ cm^{-2} from the position of the G-peak (1591 cm^{-1}) in the Raman spectrum.[22] The relatively small inhomogeneity for the suspended graphene sample mainly comes from nonuniform distribution of defects over the sample. At low THz intensity, THz transmission through graphene is spectrally flat validating the simple Drude model on which the graphene sheet conductivity is based.[11]

We have observed that intense THz pulses (the peak THz field E_{THz} exceeds 1 MV/cm) give rise to strong nonlinear transmission through the graphene samples. Figure 2(a) shows the spatially and temporally averaged THz transmission through the suspended graphene sample (blue and red lines for top and bottom holes of the sample holder, respectively) versus incident peak field amplitude. The field induced effects exhibit a threshold behavior: the transmission changes little in the low intensity region and shows an abrupt increase above 50 kV/cm. The nonlinear transmission tends to saturate in the high field regime. The spatially averaged transmission through the top hole is slightly lower than that through the bottom hole in the entire intensity range, while the differential transmission, $\Delta T/T_0 = (T - T_0)/T_0$, where T_0 is the transmission at low THz intensity, is nearly identical for both holes (Fig. 2(b)).

To better understand the nonlinear THz effect, we compare the magnitude of THz-induced transparency to the local sheet conductivity. Figure 3 shows differential transmission ($\Delta T/T_0$) images of (a) PMMA/graphene-on-Si and (b) free-standing PMMA/graphene. By increasing the incident THz field strength from 30 kV/cm to 800 kV/cm, we observed large enhancement in transmission (~10% in Fig. 3(a) and ~30% in Fig. 3(b)). The image of THz-induced transparency in the graphene-on-Si sample (Fig. 3(a-iii)) matches well with the sheet conductivity image shown in Fig. 1(a), indicating that the nonlinear THz signal is larger where the

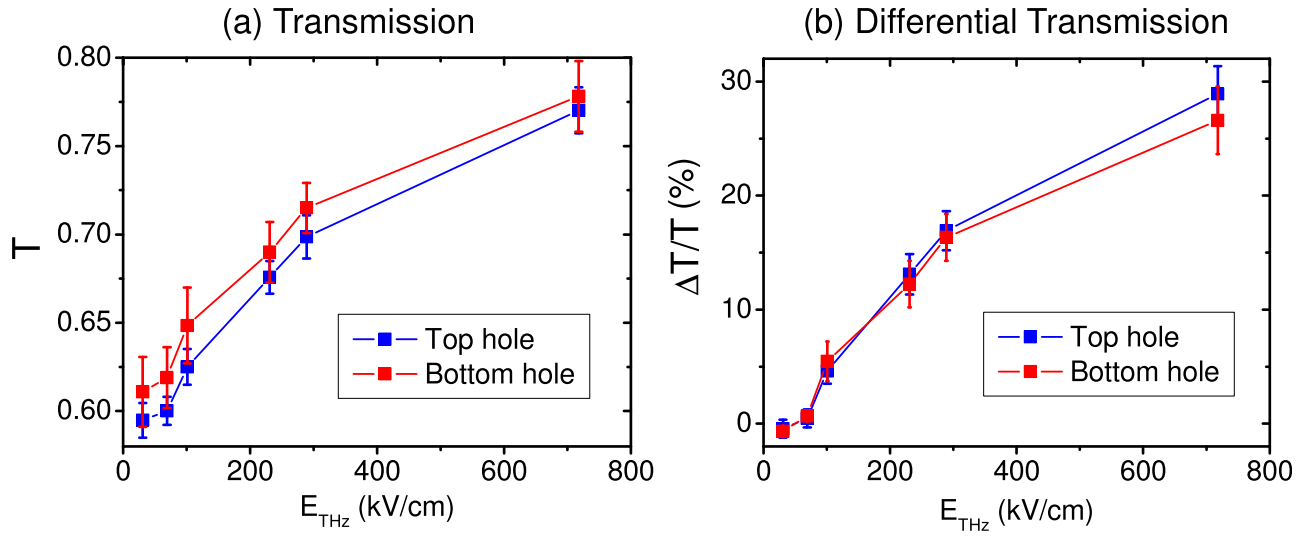

FIG. 2. (a) Spatially and temporally averaged transmission and (b) normalized differential transmission through the top (red) and bottom (black) holes of the suspended graphene sample.

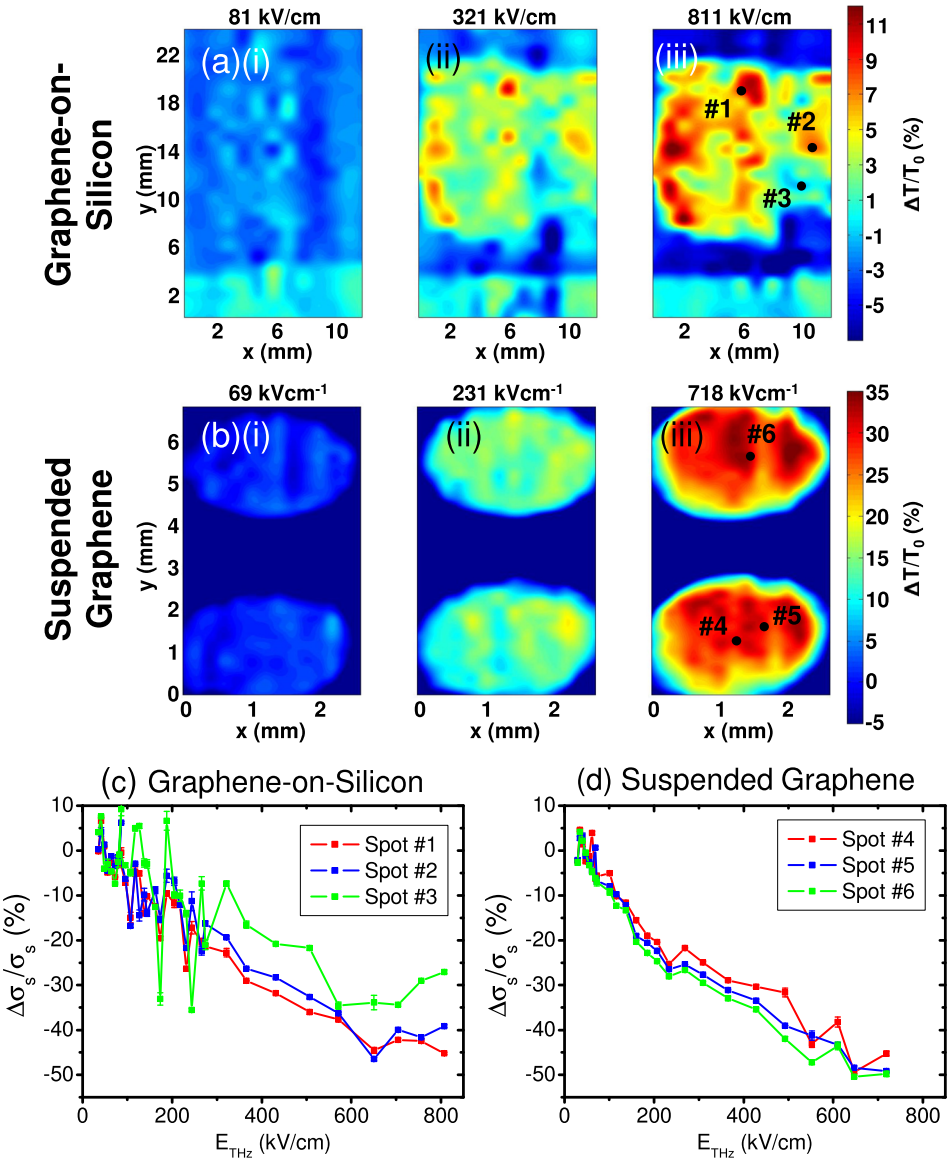

FIG. 3. Differential transmission ($\Delta T/T_0$) images taken at $E_{THz} = 80$, 300, 800 kV/cm for (a) PMMA/graphene-on-Si and (b) free-standing PMMA/graphene. (c) and (d) Time-averaged differential sheet conductivity ($\Delta\sigma_s/\sigma_s$) at three spots on each sample. The spot locations (spots #1–6) are marked in Figs. 3(a-iii) and 3(b-iii).

graphene growth coverage is more complete (spot #1: completely covered; #2: almost covered; #3: partially covered). The nonlinear THz transmission of the suspended graphene sample is largely uniform and no clear spatial correlation is found between the linear and nonlinear responses. Overall, the differential transmission in the suspended graphene sample ($\Delta T/T_0 \cong 30\%$ at 800 kV/cm) is significantly higher than that in the graphene-on-Si sample ($\Delta T/T_0 < 15\%$ at 800 kV/cm). This result demonstrates that suspended graphene is superior to graphene on a dielectric substrate for a device to manipulate THz signals.

We first discuss the apparent differences between the suspended graphene and the graphene-on-Si samples. The refractive index of the substrate affects the relationship between $t(\sigma_s)$ and σ_s (see Eq. (1)). The transmission through suspended graphene is more sensitive to σ_s than is the transmission through graphene on silicon. To account for this effect, we use Eq. (1) and the differential transmission data to calculate changes in sheet conductivity ($\Delta\sigma_s$). The normalized change in sheet conductivity ($\Delta\sigma_s/\sigma_s$) at different spots on the samples (spots #1–6 in Figs. 3(a-iii) and 3(b-iii)) is plotted in Figs. 3(c) and 3(d). It is striking that the normalized nonlinear conductivity is independent of location and consistently reaches $\sim 50\%$. This result reveals the intrinsic nonlinear THz dynamics of carriers in graphene and explains the ubiquitous intensity dependence shown in Figs. 3(c) and 3(d). Intense THz fields drive electrons into high momentum states far from equilibrium, and give rise to two competing processes to change the conductivity. First, the subsequent electron-electron scattering redistributes the occupied states in the momentum space. The redistribution of the occupied states opens up more phase space for scattering with phonons and defects, thereby reducing the scattering time and consequently lowering the conductivity. Second, the high-field interactions increase the carrier density via band-to-band transitions, effectively raising the conductivity. The scattering time increase should be dominant in the low-field regime, while the carrier density increase becomes substantial in the high-field regime and the nonlinear conductivity becomes saturated.

To investigate the time dependence of the phenomena, we measured the temporal evolution of the transmission enhancement in the graphene samples. Figure 4(a) shows the transmitted waveforms through the suspended graphene sample at different incident THz field strengths, $E_{THz} = 220$,

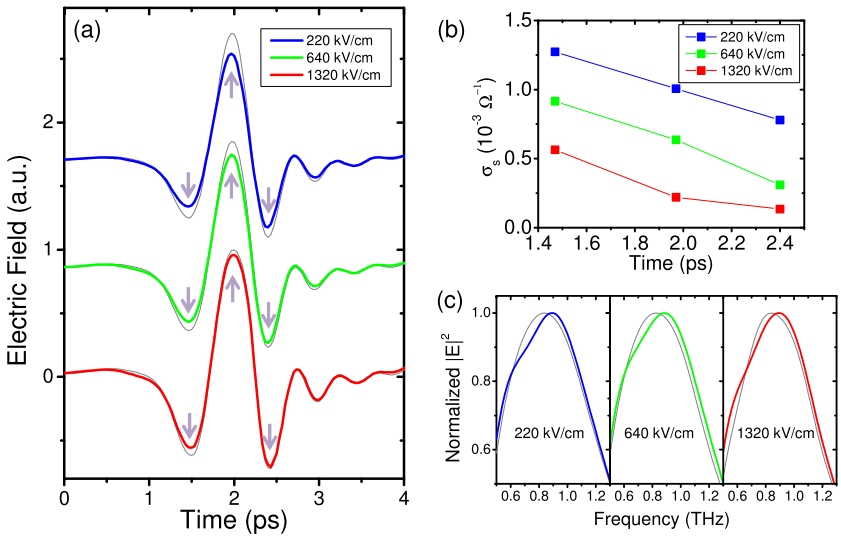

FIG. 4. (a) THz waveforms transmitted through the suspended graphene sample. The solid colored lines represent the transmission at $E_{THz} = 220$, 640, and 1320 kV/cm. The thin gray lines indicate incident pulse waveforms. (b) Transient sheet conductivity at the three peak positions, 1.5, 2.0, and 2.4 ps. (c) THz transmission spectra of the graphene sample (colored lines) in the high field regime obtained by Fourier transform of the transmitted THz waveforms. Reference spectra of the incident pulses are shown in gray lines. The spectra are normalized at the highest value.

640, and 1320 kV/cm. The thin gray lines indicate the incident pulse waveforms for comparison. Under low incident THz fields ($E_{THz} < 50$ kV cm^{-1}), the graphene layers behave like a Drude metal showing flat temporal and spectral (0.5–1.5 THz) transmission. In the high-field regime, however, the transmission gradually rises throughout the pulse duration: the transmission is relatively low in the first peak at 1.5 ps, moderate in the main peak at 2 ps, and high in the trailing peak at 2.4 ps. As the field strength increases, the dynamical behavior becomes more pronounced. It is notable that the transient transmission of the trailing peak at 2.4 ps is close to unity at the highest THz intensity, i.e., the graphene layers become almost transparent in the high-field regime. Using these data, we acquired transient sheet conductivity at the three peaks of the waveforms. Figure 4(b) shows the temporal evolution of the sheet conductivity, monotonically decreasing as the delay time increases. At the highest intensity, the sheet conductivity reduces to 0.13×10^{-3} Ω^{-1} ($\Delta\sigma_s/\sigma_s \cong 90\%$) at the trailing peak. The dynamic changes in transmission give rise to the modulations in the Fourier spectra, shown in Fig. 4(c). The spectra exhibit slight blue shifts and broadening in the high field regime due to the dynamic nonlinear THz transmission. The spectral modulation is most pronounced at the medium field strength ($E_{THz} = 640$ kV/cm), where the pulse shape undergoes the largest change, but not at the highest field strength ($E_{THz} = 1320$ kV/cm), where the fast saturation of THz-induced transparency makes relatively small changes in the pulse shape.

In conclusion, intense THz fields induce transparency in graphene by transiently decreasing its conductivity. The nonlinear THz transmission maps out the macroscopic inhomogeneity in a large-area graphene layer. The THz-induced transparency is significantly higher in the suspended graphene/PMMA film than in the graphene-on-Si sample. This result demonstrates that a THz device consisting of suspended graphene will more efficiently manipulate THz signals than one with graphene on a dielectric substrate. On the other hand, the normalized nonlinear conductivity is independent of the extrinsic sample parameters such as spatial inhomogeneity and substrate material. The nonlinear conductivity consistently reduces to 50% at a variety of locations on the two different samples. The THz-induced transparency is a dynamic process, gradually rising throughout the pulse duration.

We thank Andreas Knorr for his fruitful discussions. This work was supported by the National Science Foundation (No. DMR-1063632) and National Research Foundation of Korea Grant (No. NRF-2011-220-D00052). The work at Yonsei was supported by the National Research Foundation of Korea (NRF) grant funded by the Korean government (Nos. NRF-2011-220-D00052 and 2011-0013255).

[1]Y.-M. Lin, C. Dimitrakopoulos, K. A. Jenkins, D. B. Farmer, H.-Y. Chiu, A. Grill, and P. Avouris, Science **327**, 662 (2010).
[2]F. Xia, T. Mueller, Y.-M. Lin, A. Valdes-Garcia, and P. Avouris, Nat. Nanotechnol. **4**, 839 (2009).
[3]J. Zheng, L. Wang, R. Quhe, Q. Liu, H. Li, D. Yu, W.-N. Mei, J. Shi, Z. Gao, and J. Lu, Sci. Rep. **3**, 1314 (2013).
[4]L. Vicarelli, M. S. Vitiello, D. Coquillat, A. Lombardo, A. C. Ferrari, W. Knap, M. Polini, V. Pellegrini, and A. Tredicucci, Nat. Mater. **11**, 865 (2012).
[5]K. L. Ishikawa, New J. Phys. **15**, 055021 (2013).
[6]R. R. Nair, P. Blake, A. N. Grigorenko, K. S. Novoselov, T. J. Booth, T. Stauber, N. M. R. Peres, and A. K. Geim, Science **320**, 1308 (2008).
[7]Z. Li, E. A. Henriksen, Z. Jiang, Z. Hao, M. C. Martin, P. Kim, H. Stormer, and D. N. Basov, Nat. Phys. **4**, 532 (2008).
[8]J. Horng, C.-F. Chen, B. Geng, C. Girit, Y. Zhang, Z. Hao, H. A. Bechtel, M. Martin, A. Zettl, M. F. Crommie, Y. R. Shen, and F. Wang, Phys. Rev. B **83**, 165113 (2011).
[9]M. J. Paul, J. L. Tomaino, J. W. Kevek, T. DeBorde, Z. J. Thompson, E. D. Minot, and Y.-S. Lee, Appl. Phys. Lett. **101**, 091109 (2012).
[10]H. Choi, F. Borondics, D. A. Siegel, S. Y. Zhou, M. C. Martin, A. Lanzara, and R. A. Kaindl, Appl. Phys. Lett. **94**, 172102 (2009).
[11]J. L. Tomaino, A. D. Jameson, J. W. Kevek, M. J. Paul, A. M. van der Zande, R. A. Barton, P. L. McEuen, E. D. Minot, and Y.-S. Lee, Opt. Express **19**, 141 (2011).
[12]M. J. Paul, Y. C. Chang, Z. J. Thompson, A. Stickel, J. Wardini, H. Choi, E. D. Minot, B. Hou, J. A. Nees, T. B. Norris, and Y.-S. Lee, New J. Phys. **15**, 085019 (2013).
[13]H. Y. Hwang, N. C. Brandt, H. Farhat, A. L. Hsu, J. Kong, and K. A. Nelson, J. Phys. Chem. B **117**, 15819 (2013).
[14]S. Tani, F. Blanchard, and K. Tanaka, Phys. Rev. Lett. **109**, 166603 (2012).
[15]J. Hebling, M. C. Hoffmann, H. Y. Hwang, K.-L. Yeh, and K. A. Nelson, Phys. Rev. B **81**, 035201 (2010).
[16]D. Turchinovich, J. M. Hvam, and M. C. Hoffmann, Phys. Rev. B **85**, 201304 (2012).
[17]X. Li, W. Cai, J. An, S. Kim, J. Nah, D. Yang, R. Piner, A. Velamakanni, I. Jung, E. Tutuc, S. K. Banerjee, L. Colombo, and R. S. Ruoff, Science **324**, 1312 (2009).
[18]X. Li, C. W. Magnuson, A. Venugopal, R. M. Tromp, J. B. Hannon, E. M. Vogel, L. Colombo, and R. S. Ruoff, J. Am. Chem. Soc. **133**, 2816 (2011).

[19]J. Hebling, K.-L. Yeh, M. C. Hoffmann, B. Bartal, and K. A. Nelson, J. Opt. Soc. Am. B **25**, B6 (2008).
[20]H. Hirori, A. Doi, F. Blanchard, and K. Tanaka, Appl. Phys. Lett. **98**, 091106 (2011).
[21]Y.-G. Jeong, M. J. Paul, S.-H. Kim, K.-J. Yee, D.-S. Kim, and Y.-S. Lee, Appl. Phys. Lett. **103**, 171109 (2013).
[22]S. Pisana, M. Lazzeri, C. Casiraghi, K. S. Novoselov, A. K. Geim, A. C. Ferrari, and F. Mauri, Nat. Mater. **6**, 198 (2007).